Electronic supplementary information (ESI)

Water Detecting through Nd^{3+}-Sensitized Photon Upconversion in Core-Shell Nanoarchitecture

Daqin Chen [a,*], Min Xu [a], Ping Huang [b], Mengfan Ma [a], Mingye Ding [a], Lei Lei [c,*]

[a] College of Materials & Environmental Engineering, Hangzhou Dianzi University, Hangzhou, 310018, China

[b] State Key Laboratory of Structural Chemistry, Fujian Institute of Research on the Structure of Matter, Chinese Academy of Sciences, Fuzhou, Fujian 350002, China

[c] College of Materials Science and Engineering, China Jiliang University, Hangzhou, 310018, China

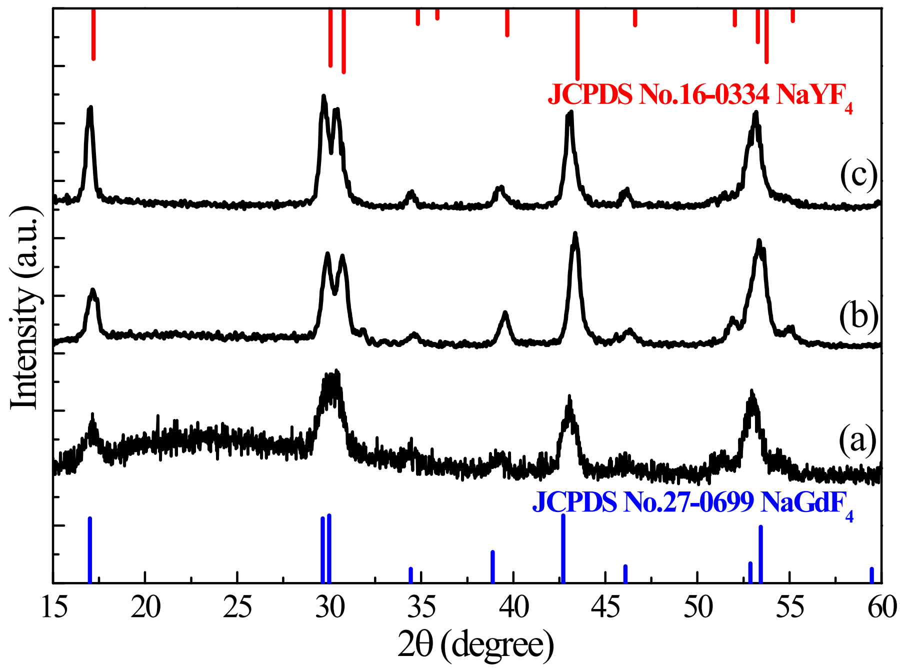

Figure S1 XRD patterns of (a) 20Yb/1Er: $NaGdF_4$ core, (b) 20Yb/1Er: $NaGdF_4$@ 20Yb/10Nd: $NaYF_4$ core-shell, (c) 20Yb/1Er: $NaGdF_4$@20Yb/10Nd: $NaYF_4$@ $NaGdF_4$ core-shell-shell samples. Bars represent standard hexagonal β-$NaYF_4$ (JCPDS No. 16-0334) and β-$NaGdF_4$ (JCPDS No. 27-0699) diffraction data, respectively.

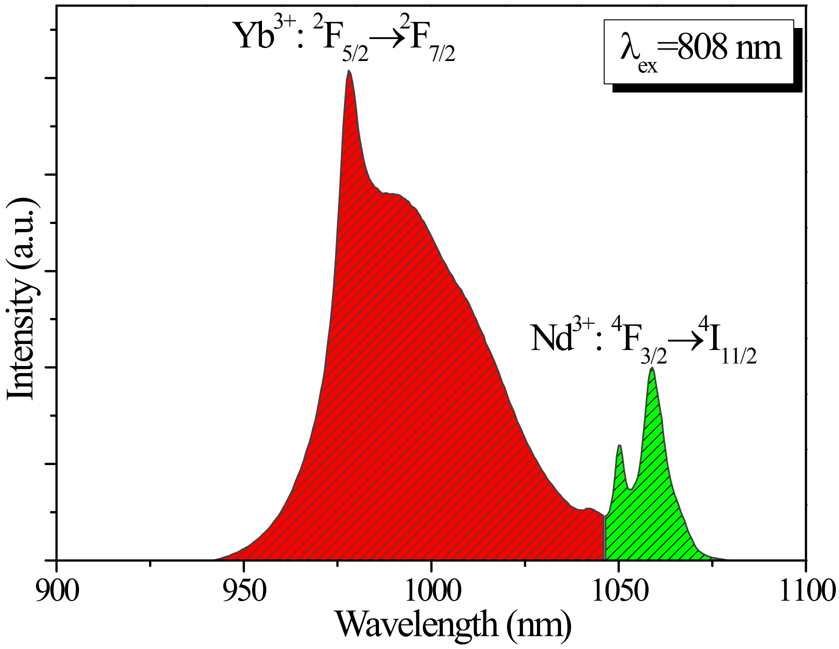

Figure S2 Photoluminescence spectrum of 20Yb/1Er:$NaGdF_4$@20Yb/10Nd:$NaYF_4$@ $NaGdF_4$ core-shell-shell sample under the excitation of 808 nm laser.

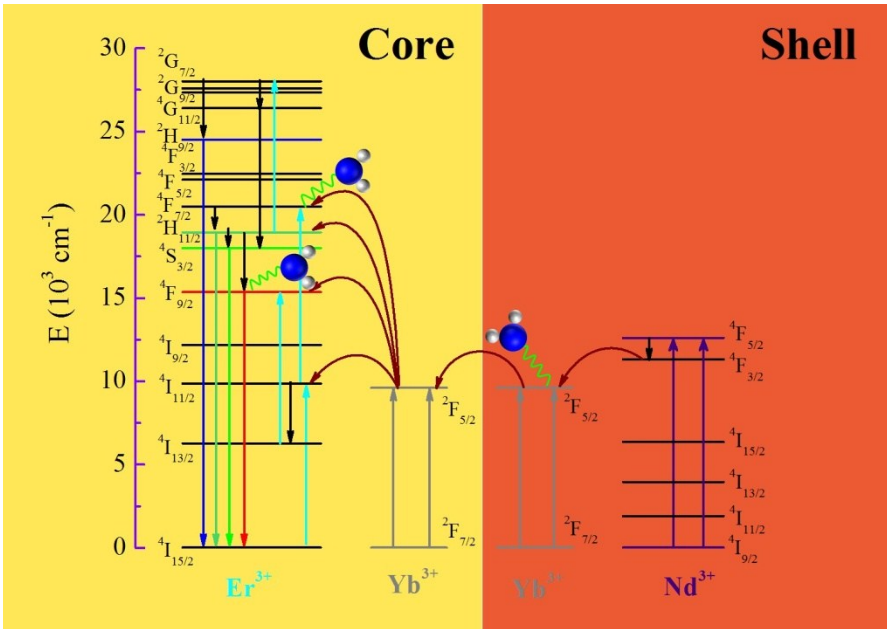

Figure S3 Energy level diagrams of Er^{3+},Yb^{3+} and Nd^{3+} ions, Nd^{3+}-sensitized UC processes as well as the proposed mechanisms for water detection under 980nm or 808 nm excitation for the present UCNCs.

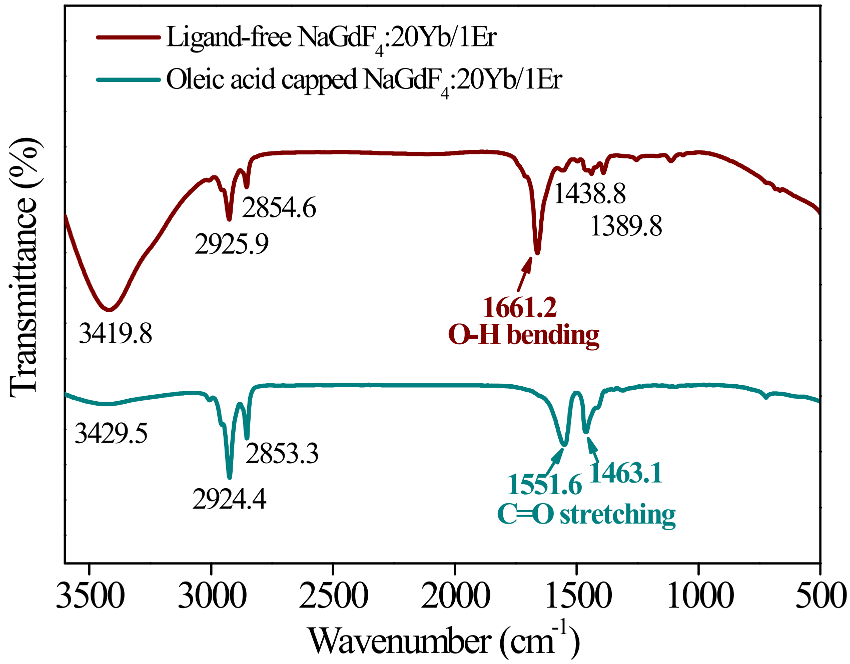

Figure S4 Fourier transform infrared spectroscopy (FTIR) of the oleic acid capped 20Yb/1Er: $NaGdF_4$ UCNCs (bottom) and the corresponding ligand-free sample (top).

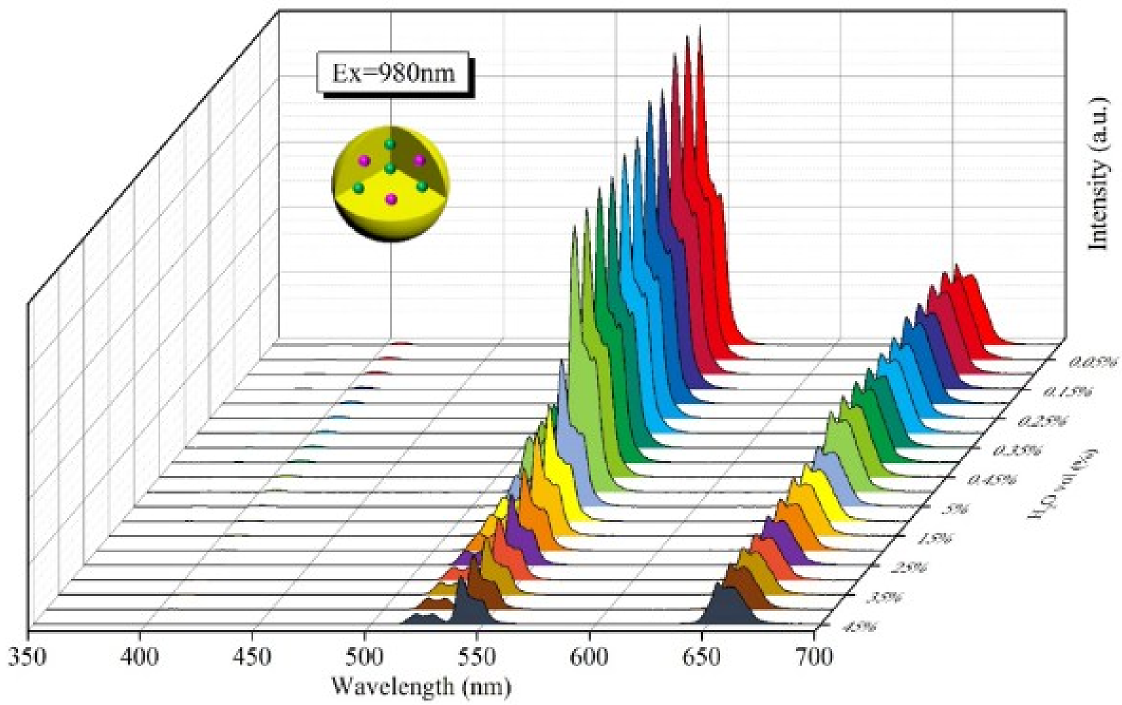

Figure S5 UC emission spectra of core UCNCs dispersed in DMF solution with different water contents under the excitation of 980 nm laser.

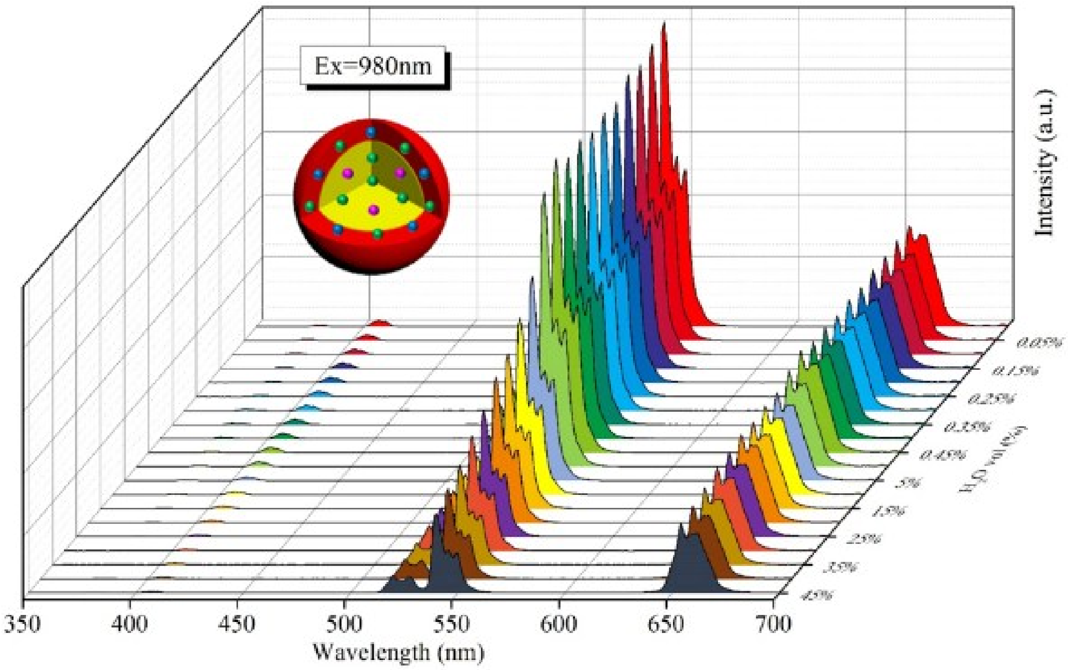

Figure S6 UC emission spectra of core-shell UCNCs dispersed in DMF solution with different water contents under the excitation of 980 nm laser.

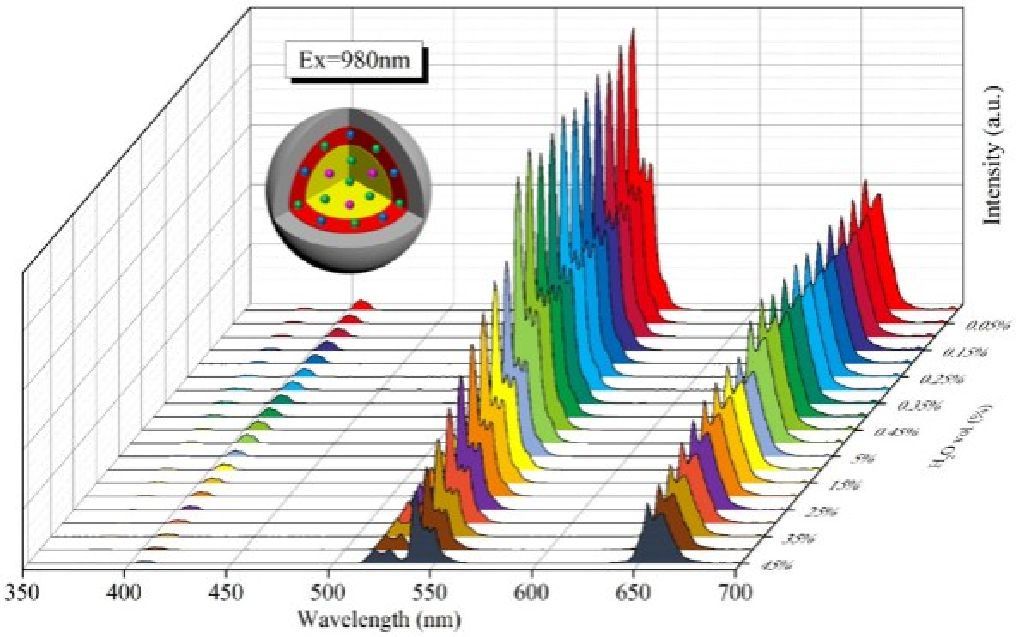

Figure S7 UC emission spectra of core-shell-shell UCNCs dispersed in DMF solution with different water contents under the excitation of 980 nm laser.

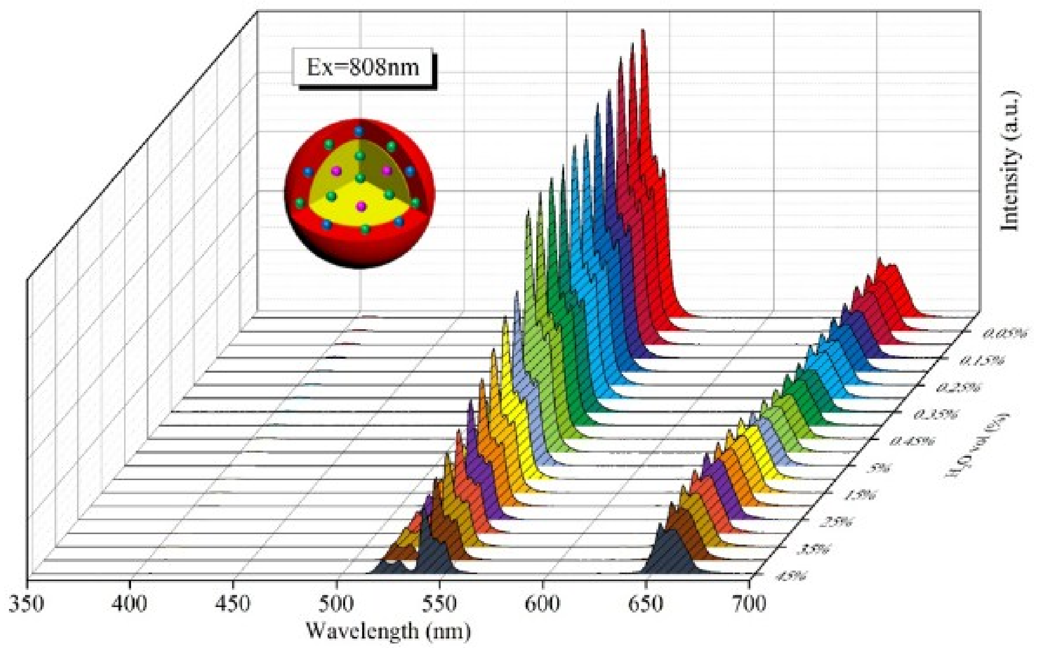

Figure S8 UC emission spectra of core-shell UCNCs dispersed in DMF solution with different water contents under the excitation of 808 nm laser.

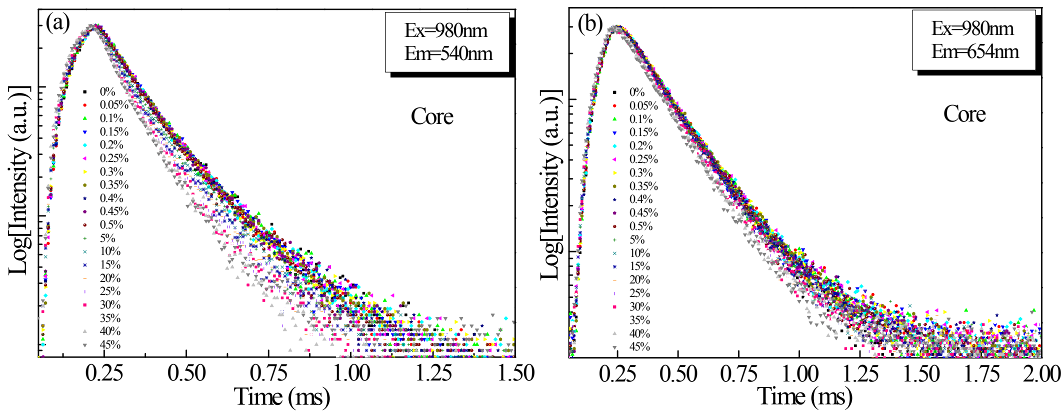

Figure S9 Water-content-dependent UC emission decay curves of (a) Er^{3+}: $^2H_{11/2}$,$^4S_{3/2}$ emitting states (λ_{em} =540 nm) and (b) $^4F_{9/2}$ one (λ_{em}=654 nm) for the core NCs under the excitation of 980 nm laser.

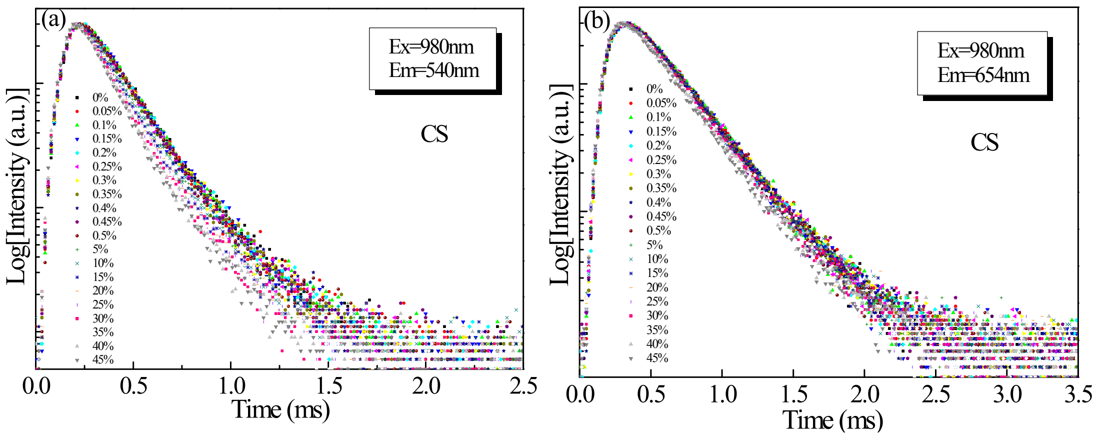

Figure S10 Water-content-dependent UC emission decay curves of (a) Er^{3+}: $^2H_{11/2}$,$^4S_{3/2}$ emitting states (λ_{em} =540 nm) and (b) $^4F_{9/2}$ one (λ_{em}=654 nm) for the core-shell NCs under the excitation of 980 nm laser.

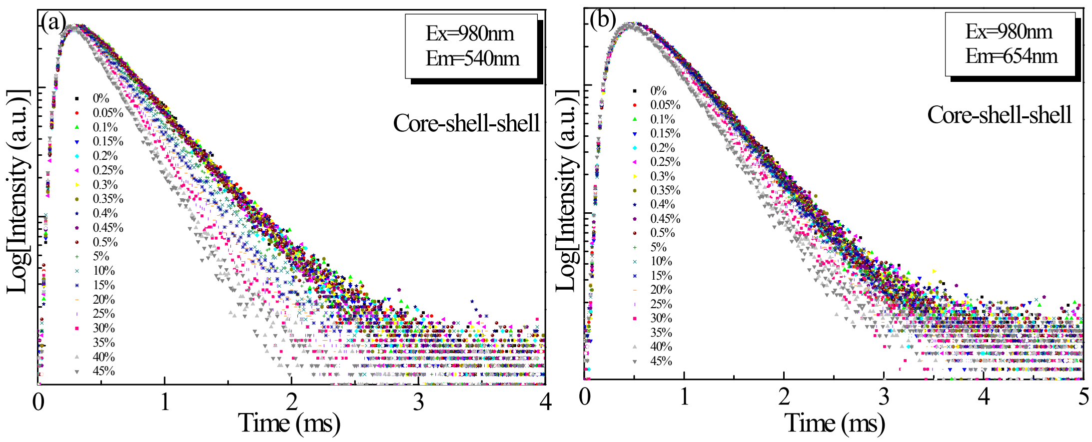

Figure S11 Water-content-dependent UC emission decay curves of (a) Er^{3+}: $^2H_{11/2}$,$^4S_{3/2}$ emitting states (λ_{em} =540 nm) and (b) $^4F_{9/2}$ one (λ_{em}=654 nm) for the core-shell-shell NCs under the excitation of 980 nm laser.

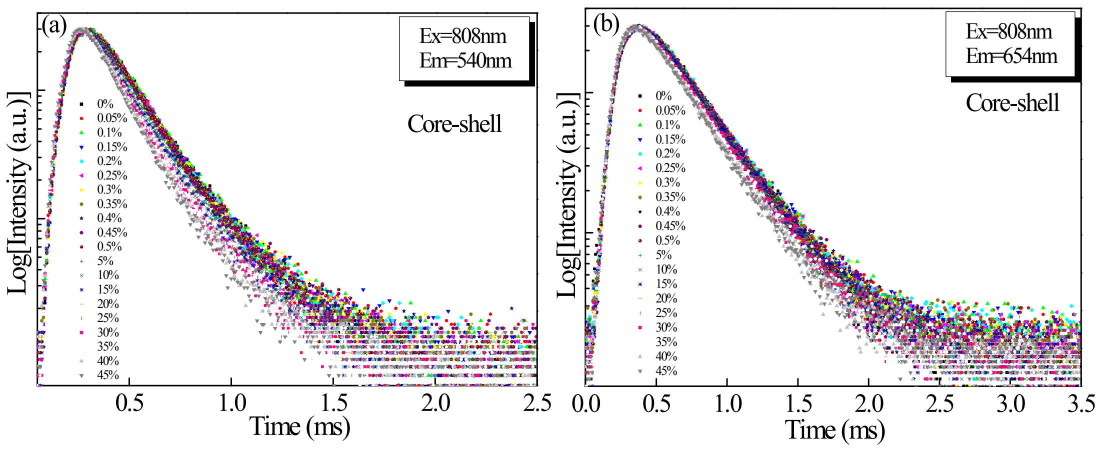

Figure S12 Water-content-dependent UC emission decay curves of (a) Er^{3+}: $^2H_{11/2}$,$^4S_{3/2}$ emitting states (λ_{em} =540 nm) and (b) $^4F_{9/2}$ one (λ_{em}=654 nm) for the core-shell NCs under the excitation of 808 nm laser.

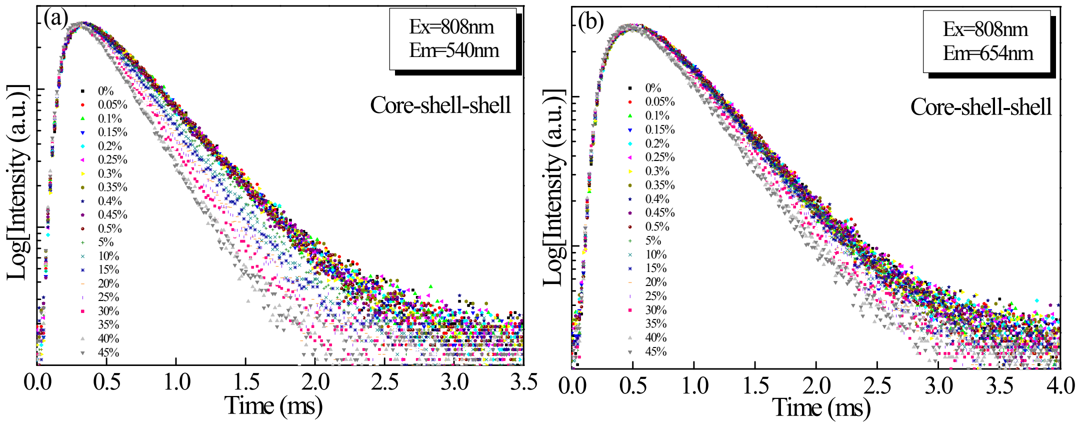

Figure S13 Water-content-dependent UC emission decay curves of (a) Er^{3+}: $^2H_{11/2}$,$^4S_{3/2}$ emitting states (λ_{em} =540 nm) and (b) $^4F_{9/2}$ one (λ_{em}=654 nm) for the core-shell-shell NCs under the excitation of 808 nm laser.

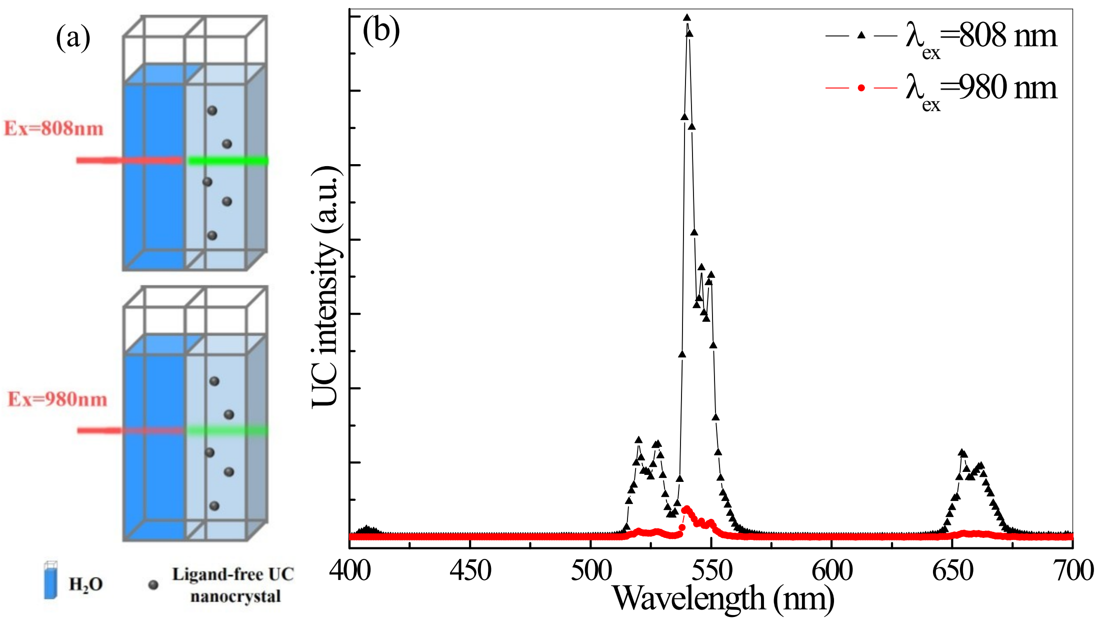

Figure S14 (a) Schematic illustrations of the noncontact method for measuring UC emission spectra under 808 nm or 980 nm laser excitation. (b) The corresponding UC emission spectra.